Sean:note everywhere I have added "the", that "upto" should be "up to", etc

Effect of Black Hole Spins on Christodoulou Memory in Binary Mergers and its implication on Observing Gravitational Wave Bursts With Memory in Pulsar Timing Array

Ashok Choudhary* and Sean T. McWilliams†
Department of Physics and Astronomy, West Virginia University, Morgantown, WV 26506, USA and
Center for Gravitational Waves and Cosmology, West Virginia University,
Chestnut Ridge Research Building, Morgantown, WV 26505, USA

The Christodoulou memory, which is a nonlinear memory effect sourced by the oscillatory component of the gravitational wave stress tensor, produces a growing, nonoscillatory change in the gravitational wave strain. This results in the permanent displacement of a pair of freely falling test masses after the gravitational wave has passed. Merger of supermassive black holes is a powerful source of gravitational wave with Chritodoulou memory effect. This effect can be potentially seen in pulsar timing observations. Initiatives to observe Burst with memory signal have assumed the signal to be a step function of a given amplitude[25], which is valid in situations like supernova explosion. But events like merger of supermassive black holes happens on the time scale of few days depending upon the mass. With future pulsar timing observation, it would be possible to see the change in Chritodoulou memory over two weeks interval of time. We investigate how the effect of Spin changes the timing residuals over a two weeks period of interval. Since Chritodoulou memory is an accumulated effect during the entire history of the source and while memory contribution during the early inspiral is well described by the post-Newtonian (PN) approximation, the contribution at merger must be obtained using numerical relativity simulations. The corrections up to third PN order (i. e. 3PN) for the gravitational wave memory from pairs of nonspinning black holes on quasicircular orbits has been computed by Favata [1]. Here we include the contribution from the individual black-hole spins at leading order which appears at 1.5PN *Sean:what is leading order here, if we then say the memory is 3PN?* and calculate the memory effect up to 3PN order. We also compute the memory contribution during the merger by using the methods presented in [1] to calculate the memory content using the oscillatory radiation as input, and applying that method using publicly available numerical relativity simulations of spinning binaries. We Finally use this model to compute the timing residuals for a memory growth during two weeks interval of time following the method described in [25]

I. INTRODUCTION

Gravitational waves (GW), when they pass through a pair of freeling falling test masses, induce an oscillatory motion. This motion is incredibly small for astrophysical sources. Nonetheless, the signals generated by ten black-hole binaries and one neutron-star binary were detected by the Advanced LIGO and Advanced Virgo[2] *Sean:cite the catalog paper*. For sources whose strength changes significantly with time, such as the final merger of compact binaries like those that have already been observed, there is an additional non-oscillatory signal that results in a permanent displacement of freely falling test masses. This permanent displacement, which is called the Christodoulou memory effect [3], is sourced by the oscillatory part of the signal, and is therefore a fundamental manifestation of nonlinearity in general relativity. This memory effect accumulates over the entire history of the source. *Ashok:This nonlinear memory effect is distinct from linear memory, which arises from the non-oscillatory motion of unbounded source Sean:give a more specific definition. Ashok:The linear memory is important for unbound astrophysical systems and have been studied in context of supernova explosions resulting in neutron star kicks [4][5]Sean:put one or more citations after each item, asymmetric mass loss due to neutrino emission [6] Sean:isn't this also in the context of supernovae? if not, what source is this?, and gamma-ray-burst jets [7–9].*

Sean:I commented out the detailing of linear memory, since the paper is about nonlinear. The above mention of linear is sufficient.

Christodoulou memory arises from a change in the radiative multipole moment, and is therefore sourced by the energy flux of radiated GWs. It can be understood by considering Einstein's equation in the harmonic gauge, and calculating the leading order nonlinear contribution. The resulting wave equation for the spacetime metric can be expressed as [10]

$$\Box\bar{h}^{\alpha\beta} = -16\pi(-g)(T^{\alpha\beta} + t_{LL}^{\alpha\beta}) - \bar{h}^{\alpha\mu}_{,\nu}\bar{h}^{\beta\nu}_{,\mu} + \bar{h}^{\mu\nu}\bar{h}^{\alpha\beta}_{,\mu\nu} \tag{1a}$$

$$\bar{h}^{\alpha\beta}{}_{,\beta} = 0 \tag{1b}$$

where

$$\bar{h}^{\alpha\beta} = \eta^{\alpha\beta} - \sqrt{-g}g^{\alpha\beta} \tag{2}$$

is the gravitational field tensor, g is the determinant of the metric $g_{\alpha\beta}$, $T^{\alpha\beta}$ is the matter stress-energy tensor, $t_{LL}^{\alpha\beta}$ is the Landau-Lifshitz pseudotensor, $\Box \equiv -\partial_t^2 + \nabla^2$ is the d'Alembertian, a comma denotes a partial derivative ($_{,\mu} \equiv \partial_\mu$), and ∇^2 is the flat-space Laplacian.

This wave equation has several source terms. The Landau-Lifshitz term represents the contribution of GWs to the stress tensor, and therefore serves as the source of the nonlinear memory contribution to GW waveform [11], *Sean:You appear to change the meanings of T and t, which you shouldn't do, but please verify that my correction is what you actually meant. Also, since the contravariant form appears in the above equation, you should give that here, rather than the covariant form.*

$$t_{LL}^{jk} \equiv \frac{1}{32\pi}\langle h_{TT}^{ab,j} h_{TT}^{ab,k}\rangle \approx t_{LL}^{00} n^j n^k = \frac{1}{R^2}\frac{dE^{gw}}{dtd\Omega} n^j n^k \tag{3}$$

* aschoudhary@mix.wvu.edu
† sean.mcwilliams@mail.wvu.edu

where TT refers to the transverse-traceless gauge, $\frac{dE^{gw}}{dtd\Omega}$ is the GW energy flux, n_j is a unit radial vector, the angle-brackets correspond to an average over several wavelengths, *Sean:what does this last one mean?* $h^{TT}_{ab} = \bar{h}^{TT}_{ab}$. The standard procedure to solve a wave equation with a source is to use the Green's function. When this approach is applied to Eq. 1a, we obtain a correction term to the gravitational field sourced by the Landau-Lifshitz term, given by [12]

$$\delta h^{TT}_{jk} = \frac{4}{R}\int_{-\infty}^{T_R} dt' \left[\frac{dE^{gw}}{dt' d\Omega'}\frac{n'_j n'_k}{(1-\boldsymbol{n'}\cdot\boldsymbol{N})}d\Omega'\right]^{TT} \tag{4}$$

where T_R is the retarded time. Eq. 4 is the nonlinear Landau-Lifshitz pseudotensor describing gravitational wave memory [3, 13, 14]. The nonlinear memory occurs in any system that radiates GWs, whereas these systems are usually considered to have a vanishing linear memory, although we can apply the formalism for linear memory to nonlinear memory if we consider the radiated gravitons to be the unbound masses [15].

The Christodoulou memory effect arises from nonlinear interactions at 2.5PN order, but it affects the GWs at leading (0PN) order. In the transverse-traceless gauge, the + polarization of the GW signal no longer oscillates around zero when memory is included, but instead accumulates a nonzero drift that remains small compared to the amplitude of the oscillatory contribution to the GWs throughout the inspiral, and becomes largest during the final merger. We can use PN methods to model the slow growth of memory during the inspiral phase, but the largest memory contribution that occurs during the merger requires information from numerical relativity (NR), since the PN approach breaks down at that stage. In principle, the memory can be extracted directly from NR simulations. However, it is challenging to extract the memory accurately. NR simulations can most accurately compute the $(l, m) = (2, 2)$ mode of the waveform, but the nonlinear memory is present in only $m = 0$ mode. These $m = 0$ modes are much smaller in magnitude and can be masked by numerical noise as well as subtleties of the numerical techniques used to extract the radiation. For a detailed discussion of these issues, see section V in reference [1] *Ashok:The Christodoulou memory from spinning binaries have been studied by Reisswig and Pollney [16] in numerical simulations, where they carry out fully relativistic binary BH simulations to directly measure the non-linear GW memory through inspiral, merger and ringdown in a gauge invariant way. In these studies, the authors have considered the equal mass spinning case, where the memory is contained in the ${}_{-2}Y_{l0}$ spin-weighted spherical harmonic components of the GW strain, h_+. The authors have found that the largest nonlinear memory is observed in case of merger of the aligned, maximally spinning BHs. Another interesting results in their studies is the case of the merger of maximally spinning anti aligned BHs, where they observed the strongest oscillating ringdown signal.*

NR simulations that use the most widely adopted methods directly compute the Weyl curvature scalar, Ψ_4, and decompose its values at large radii R into a sum over spin-weighted spherical harmonic modes:

$$\Psi_4 = \ddot{h}_+ - i\ddot{h}_\times = \sum_{l=2}^{\infty}\sum_{m=-l}^{l} \psi_{lm}(t,R)\,{}_{-2}Y_{lm}(\Theta,\Phi) \tag{5}$$

In terms of the ψ_{lm} modes, the leading-order Christodoulou-memory modes are smaller than the ψ_{22} modes by *five* PN orders. The relative mode magnitudes([1]) are $\psi_{22} \approx 690\psi_{20} \approx 4.5\times10^4\psi_{40}$ at $x \approx 1/5$. There are other difficulties too in calculating memory from NR data. Construction of the h_{lm} from ψ_{lm} requires two integration constants to be specified. Choosing these integration constant to be zero [17] does not make the signal oscillate around zero. Although it should not if memory is present, but this nonlinear growth is not solely due to actual memory effect. This can also be caused by numerical noise. So there is an artificial memory in the h_{lm} modes which is caused by numerical noise. This artificial memory is unphysical and arises from the finite size of the initial separation and extraction radius. The initial burst of junk radiation also contribute to artificial memory.

NR simulations starts at a finite radius, so although it contains most part of gravitational wave memory, PN results should be used for early inspiral phase. The significance of memory accumulated during the inspiral phase can be seen by looking at the largest memory mode h_{20}. Consider the leading-(Newtonian)-order piece of the largest memory mode h_{20}:

$$h^{NR}_{20}(T_R) = \frac{1}{\sqrt{2}R}\int_{T_0}^{T_R} U^{(mem)(1)}_{20}(t)dt \tag{6}$$

where $U^{(mem)(1)}_{20}$ is given by the leading order piece of Eq. (3.13a) in ref [1], and the T_0 is the starting time of the simulation. For a realistic, quasicircular binary that inspirals from a large initial separation, $T_0 \to -\infty$. The NR simulations of binaries that starts at a finite initial separation would underestimate the size of the memory. For a simulation that starts with an initial separation of $10M$, the error in the memory at a harmonic coordinate separation of $5M$ is 50%.[1]

The corrections to the leading-oder formula for the nonlinear memory's contribution to 3PN order for non-spinning binaries has been computed by by Favata [1]. However the effect of binary spins have not been explored in these results. Astrophysical black holes are formed by gravitation collapse of massive star when when they run out of their nuclear fuel in the core. These massive stars are likely to posses spin angular momentum, as a result the black hole formed would also be spinning. The black holes can also accrete matter from surrounding and as a result spin up during the process. It is highly likely that there is a large population of spinning binaries in the universe.

In this paper we calculate the nonlinear memory contribution to the + waveform polarization and look at the effect of spin contribution. For PN calculations, this paper is just an extension of Favata's[1] paper, where we include the spin contribution up to leading (1.5 PN) order for nonprecessing binaries. The nonlinear memory contribution near merger is computed using NR data from publicly available SXS catalog, where we process the data to remove the low frequency numerical noise. In Sec. II, we describe the calculation required to compute memory contribution to the post-Newtonian waveform of quasi-circular, inspiralling binaries. In Sec. III, we describe the method used to extract memory contribution from NR simulations. Sec. IV we give the results which looks at the effect of spin on total nonlinear memory. We use PN expressions for memory for early time and for late time we use memory extracted from NR simulations.

II. MEMORY CONTRIBUTION TO POST-NEWTONIAN WAVEFORM POLARIZATION

The mode decomposition in terms spin-weighted spherical harmonics for gravitational wave polarization is given by

$$h_+ - ih_\times = \sum_{l=2}^{\infty}\sum_{m=-l}^{m=l} h^{lm}\,{}_{-2}Y^{lm}(\Theta,\Phi) \tag{7}$$

where ${}_{-2}Y^{lm}$ are spin-weighted spherical harmonics, the angles (Θ,Φ) indicates the direction from the source to the observer. In a multipolar expansion of the GW field, the modes h^{lm} are related to the radiative mass U^{lm} and the current V^{lm} multipole via

$$h^{lm} = \frac{G}{\sqrt{2}\,R}\left[U^{lm}(T_R) - \frac{i}{c}V^{lm}(T_R)\right] \tag{8}$$

Here R is the distance from source to observer, T_R is retarded time. We assume $c = G = 1$ for all out calculations. The spin weighted spherical harmonics are defined in terms of the Wigner d function by

$${}_{-2}Y^{lm}(\Theta,\Phi) = (-1)^2\sqrt{\frac{2l+1}{4\pi}}d^l_{ms}(\Theta)e^{im\Phi} \tag{9}$$

Here

$$d^l_{ms} = \sqrt{(l+m)!(l-m)!(l+s)!(l-s)!} \tag{10}$$

$$\times\sum_{k=k_i}^{k_f}\frac{(-1)^k(\sin\frac{\Theta}{2})^{2k+s-1}(\cos\frac{\Theta}{2})^{1l+m-s-2k}}{k!(l+m-k)!(l-s-k)!(s-m+k)!} \tag{11}$$

where $k_i = \max(0, m-s)$ and $k_f = \min(l+m, l-s)$.
When the GW field is decomposed into spin-weighted spherical harmonic modes, the nonlinear memory can be shown to yield a correction to the radiative mass multipole moments that enters at 2.5PN and higher orders. For more detail about GW multipole expansion [10]. The correction to the radiative mass multipole moments is given by

$$U^{(mem)}_{lm} = 32\pi\frac{(l-2)!}{2(l+2)!}\int_{-\infty}^{T_R}dt\int d\Omega\frac{dE_{gw}}{dtd\Omega}(\Omega)Y^*_{lm}(\Omega) \tag{12}$$

The radiative current moments V_{lm} do not contribute to nonlinear memory. The GW energy flux can be computed from the GW stress-energy tensor and is given by [18]

$$\frac{dE_{gw}}{dtd\Omega} = R^2T^{gw}_{00} = \frac{R^2}{32\pi}\langle\dot{h}^{TT}_{jk}\dot{h}^{TT}_{jk}\rangle = \frac{R^2}{16\pi}\langle\dot{h}^2_+ + \dot{h}^2_\times\rangle \tag{13}$$

where the angled bracket mean to average over several wavelengths. The energy flux can be written in terms of h_{lm} modes using equation 7 in the following way:

$$\frac{dE_{gw}}{dtd\Omega} = \frac{R^2}{16\pi}\sum_{l'=2}^{\infty}\sum_{l''=2}^{\infty}\sum_{m'=-l'}^{l'}\sum_{m''=-l''}^{l''}\langle\dot{h}_{l'm'}\dot{h}^*_{l''m''}\rangle\,{}_{-2}Y^{l'm'}(\theta,\phi)\,{}_{-2}Y^{l''m''*}(\theta,\phi) \tag{14}$$

The memory contribution to the mass multipole moment can now be evaluated using equation 12 and 14. The angular part of the integral has the following form

$$\int d\Omega\,{}_{-2}Y_{l'm'}(\theta,\phi)\,{}_{-2}Y^*_{l'm''}(\theta,\phi)Y^*_{lm}(\theta,\phi) \tag{15}$$

The above integral can be evaluated as done in section III of Favata[1]. The results are also shown in appendix A. The time derivative of the memory mass-multipole moment is defines as $U^{(mem)(1)}_{lm} \equiv \frac{dU^{(mem)}_{lm}}{dT_R}$ [1], which when combined using equation 12 and 14 and Appendix A, can be written as

$$U^{(mem)(1)}_{lm} = R^2\sqrt{\frac{2(l-2)!}{(l+2)!}}\sum_{l'=2}^{\infty}\sum_{l''=2}^{\infty}\sum_{m'=-l'}^{l'}\sum_{m''=-l''}^{l''}(-1)^{m+m'} \times\left\langle\dot{h}_{l'm'}\dot{h}^*_{l'm'}\right\rangle G^{2-20}_{l'm'lm'-m''-m} \tag{16}$$

where $G^{2-20}_{l'm'lm'-m''-m}$ is the angular integral of equation 15 and is given in Appendix A. The above equation can be used to compute the first time derivative of mass-multipole moment by substituting the GW modes h_{lm}. When evaluating equation 16, we are only interested in $m = 0$ modes. The $m \neq 0$ terms yield oscillatory contribution to the waveform polarizations that enter at higher PN orders then the nonoscillatory, $m = 0$ terms. The non-vanishing, non-oscillatory modes are $U^{(mem)}_{l0}$ with l-even. These $U^{(mem)}_{l0}$ consist of time-integral of polynomials in $x \equiv (M\omega)^{2/3}$ (where ω is the orbital angular frequency), with each terms of the form

$$\int_{-\infty}^{T_R}x^n dt = \int_{-\infty}^{T_R}\frac{x^n}{\dot{x}}dx \tag{17}$$

After performing the change of variable indicated in above equation 17, evaluation of the resulting integrals requires a model for the frequency evolution of the binary. The adiabatic evolution of the frequency (or x) is easily derived from energy balance ($\mathcal{L}_{GW} = -\dot{E}$). and the relation $\dot{x} = -\mathcal{L}_{GW}/(dE/dx)$. The 3.5PN orbital energy and flux are given in Appendix C of reference [19]. Here we show only up to 1.5 PN terms, the complete expression are show in Appendix C1. The 1.5 PN expression for energy is given by

$$E = -\frac{\eta M x}{2}\left\{1 + x\left[-\frac{3}{4} - \frac{\eta}{12}\right] + x^{3/2}\left[\left(\frac{8}{3} - \frac{4\eta}{3}\right)\boldsymbol{\chi}_s \cdot \hat{\mathbf{L}}_N + \frac{8}{3}\delta\boldsymbol{\chi}_a \cdot \hat{\mathbf{L}}_N\right]\right\} \tag{18}$$

and the 1.5 PN GW luminosity is given by

$$\mathcal{L} = \frac{32}{5}\eta^2 x^5\left\{1 + x\left[-\frac{1247}{336} - \frac{35\eta}{12}\right] + x^{3/2}\left[4\pi - \left\{\left(\frac{11}{4} - 3\eta\right)\boldsymbol{\chi}_s \cdot \hat{\mathbf{L}}_N + \frac{11}{4}\delta\boldsymbol{\chi}_a \cdot \hat{\mathbf{L}}_N\right\}\right]\right\} \tag{19}$$

Substituting the above two equation into $\dot{x} = -\mathcal{L}_{GW}/(dE/dx)$, and expanding up to 1.5 PN gives the following expression.

$$\frac{dx}{dt} = \frac{64\,x^5\,\eta}{5}\left\{1 + x\left[-\frac{743}{336} - \frac{11\eta}{4}\right] + x^{3/2}\left[4\pi - \frac{113}{12}\delta\,\boldsymbol{\chi}_a \cdot \hat{\mathbf{L}}_N - \left(-\frac{113}{19} + \frac{19\,\eta}{3}\right)\boldsymbol{\chi}_s \cdot \hat{\mathbf{L}}_N\right]\right\} \tag{20}$$

The results up to 3.5 PN are shows in Appendix C. The equation 20 can be used to change the integration with respect to time into integration with respect to x as shown in equation in 17. The expressions for h_{lm} whose first time derivatives appear equation 16 can be obtained from Ref[19]. The GW modes for precessing binaries with small inclination angle on nearly circular orbits through 1.5 PN order are given in section IV of ref [19]. Setting $\iota = 0, \alpha = \pi$ in equation 4.16 and 4.17 gives the result for non-precessing case. In our case the spins are aligned along z axis, so we set $\chi_a^x = \chi_s^x = \chi_a^y = \chi_s^y = 0$. We can now write the expression as

$$h_{lm} = (-1)^{m+1}\frac{(2M\eta x)}{D_L}\sqrt{\frac{16\pi}{5}}e^{im\psi}\hat{h}_{lm}, \tag{21}$$

and $\hat{h}_{lm}$ modes are given by

$$\hat{h}_{22} = 1 + x\left(-\frac{107}{42} + \frac{55\eta}{42}\right) + x^{3/2}\left(2\pi - \frac{4\,\delta\,\chi_a^z}{3} + \frac{4}{3}(-1+\eta)\chi_s^z\right) \tag{22a}$$

$$\hat{h}_{21} = \frac{i\delta}{3}\left[x^{1/2} - x\frac{3}{2\delta}(\chi_a^z + \delta\chi_s^z) + x^{3/2}\left(-\frac{17}{28} + \frac{5\eta}{7}\right)\right] \tag{22b}$$

$$\hat{h}_{32} = \frac{9}{8}\sqrt{\frac{5}{7}}\left[\frac{8}{27}x(1-3\nu) + \frac{32}{27}x^{3/2}\eta\chi_s^z\right] \tag{22c}$$

The remaining h_{lm} expressions does not contain spin terms and the complete expressions up to 3PN terms can be directly taken from Ref.[20] We show the h_{lm} expressions for positive m values, but the results for negative m values can be obtained by the relation, $h_{l,-m} = (-1)^l\bar{h}_{lm}$. This results is not in general true for precessing binaries, but it continues to hold true of non-precessing case. The time derivative of h_{lm} modes can be obtained by following the procedure shown in Appendix B. With these modes we use equation 16 to evaluate the first time derivative of the memory mass-multipole moment, which is further integrated using equation 17. The results after integration are show in next section.

A. RESULTS: MEMORY CONTRIBUTION TO THE POST-NEWTONIAN WAVEFORM OF QUASI-CIRCULAR, INSPIRALLING BINARIES

The memory contribution to the spin-weighted spherical-harmonic modes of the polarization waveform [Eq. 8]. These quantities are related via

$$h_{l0}^{(mem)} = \frac{\alpha}{\sqrt{2}\,R}U_{l0}^{(mem)} = 8\sqrt{\frac{\pi}{5}}\frac{\eta M x}{R}\hat{H}_{lm} \tag{23}$$

where we have followed the notation of Sec. 9 of Ref. [20]. The parameter α takes the value as shown below, depending upon the polarization triad chosen.

$$\alpha = \begin{cases} (+1) & \text{for the Kidder [21] convention} \\ (-1) & \text{for the Blanchet et al. [20] convention} \end{cases} \tag{24}$$

The results of polarization modes in terms of $\hat{H}_{l0}$ are:

$$\hat{H}_{20} = \alpha\frac{5}{14\sqrt{6}}\left\{1 + x\left[-\frac{4075}{4032} + \frac{67\,\eta}{48}\right] + x^{3/2}\left[\left(\frac{7}{480} + \frac{27\,\delta}{10} - \frac{7\,\eta}{120}\right)\boldsymbol{\chi}_a \cdot \hat{\mathbf{L}}_N + \left(\frac{27}{10} + \frac{7\,\delta^3}{480} - \frac{2\,\eta}{15}\right)\boldsymbol{\chi}_s \cdot \hat{\mathbf{L}}_N\right]\right.$$

$$
\begin{aligned}
&x^2\left[-\frac{151877213}{67060224}-\frac{123815\,\eta}{44352}+\frac{205\,\eta^2}{352}+\left(-\frac{163}{96}+\frac{161\,\eta}{24}\right)\boldsymbol{\chi}_a^2+\left(-\frac{27\,\delta}{8}-\frac{\delta^3}{48}\right)\boldsymbol{\chi}_s\cdot\boldsymbol{\chi}_a+\left(-\frac{27}{16}-\frac{\delta^4}{96}-\frac{\eta}{12}\right)\boldsymbol{\chi}_s^2\right]\\
&x^{5/2}\left[-\frac{253\,\pi}{336}+\frac{253\,\pi\,\eta}{84}+\left\{\frac{631}{32256}+\frac{788471\,\delta}{84672}+\left(-\frac{5}{126}-\frac{991\,\delta}{1008}\right)\eta-\frac{311\,\eta^2}{2016}\right\}\boldsymbol{\chi}_a\cdot\hat{\mathbf{L}}_N\right.\\
&\quad\left.+\left\{\frac{788471}{84672}-\frac{631\,\delta^3}{32256}-\left(-\frac{36509}{2646}+\frac{311\,\delta^3}{8064}\right)\eta+\frac{853\,\eta^2}{252}\right\}\boldsymbol{\chi}_s\cdot\hat{\mathbf{L}}_N\right]\\
&x^3\left[-\frac{4397711103307}{532580106240}+\left(\frac{700464542023}{13948526592}-\frac{205\,\pi^2}{96}\right)\eta+\frac{69527951\,\eta^2}{166053888}+\frac{1321981\,\eta^3}{5930496}-\left(-\frac{7\,\pi}{256}+\frac{275\,\pi\,\delta}{12}\right.\right.\\
&\quad\left.\frac{7\,\pi\,\delta}{256}\right)\boldsymbol{\chi}_a\cdot\hat{\mathbf{L}}_N+\left\{-\frac{42787}{32256}+\frac{791\,\delta}{9216}+\frac{113\,\delta^2}{576}+\left(\frac{354035}{32256}-\frac{791\,\delta}{2304}\right)\eta-\frac{2533\,\eta^2}{128}\right\}\boldsymbol{\chi}_a^2\\
&\quad\left\{\frac{275\,\pi}{12}-\frac{7\,\pi\,\delta^3}{256}-\frac{56\,\pi\eta}{3}+\left(\frac{791}{9216}-\frac{47869\,\delta}{21504}-\frac{743\,\delta^3}{21504}+\frac{791\,\delta^4}{9216}+\left(-\frac{77}{192}+\frac{87269\,\delta}{2304}-\frac{11\,\delta^3}{256}\right)\eta+\frac{133\,\eta^2}{576}\right)\boldsymbol{\chi}_a\cdot\hat{\mathbf{L}}_N\right\}\boldsymbol{\chi}_s\cdot\hat{\mathbf{L}}_N\\
&\quad\left.\left\{-\frac{47869}{43008}+\frac{791\,\delta^3}{9216}-\frac{743\,\delta^4}{43008}+\left(\frac{57677}{1792}-\frac{133\,\delta^3}{2304}-\frac{11\,\delta^4}{512}\right)\eta-\frac{15029\,\eta^2}{1152}\right\}\boldsymbol{\chi}_s^2\right]\Big\}
\end{aligned}
\tag{25a}
$$

$$
\begin{aligned}
\hat{H}_{40}=\alpha\frac{1}{504\sqrt{2}}\Bigg\{&1+x\left[-\frac{180101}{29568}+\frac{27227\,\eta}{1056}\right]+x^{3/2}\left[\left(\frac{7}{40}+\frac{27\,\delta}{10}-\frac{7\,\eta}{10}\right)\boldsymbol{\chi}_a\cdot\hat{\mathbf{L}}_N+\left(\frac{27}{10}+\frac{7\,\delta^3}{40}+\frac{46\,\eta}{5}\right)\boldsymbol{\chi}_s\cdot\hat{\mathbf{L}}_N\right]\\
&x^{5/2}\left[-\frac{13565\,\pi}{1232}+\frac{13565\,\pi\,\eta}{308}+\left\{\frac{379}{2688}-\frac{1457321\,\delta}{68992}+\left(-\frac{59}{336}+\frac{3094367\,\delta}{22176}\right)\eta-\frac{87\,\eta^2}{56}\right\}\boldsymbol{\chi}_a\cdot\hat{\mathbf{L}}_N\right.\\
&\quad\left.\left\{-\frac{1457321}{68992}+\frac{379\,\delta^3}{2688}+\left(\frac{5892749}{38808}+\frac{87\,\delta^3}{224}\eta-\frac{469813\,\eta^2}{5544}\right)\right\}\boldsymbol{\chi}_s\cdot\hat{\mathbf{L}}_N\right]\\
&x^2\left[\frac{2201411267}{158505984}-\frac{34829479\,\eta}{432432}+\frac{844951\,\eta^2}{27456}+\left(-\frac{85}{48}+7\,\eta\right)\boldsymbol{\chi}_a^2+\left(-\frac{27\,\delta}{8}-\frac{\delta^3}{6}\right)\boldsymbol{\chi}_s\cdot\boldsymbol{\chi}_a+\left(-\frac{27}{16}-\frac{\delta^4}{12}+\frac{\eta}{12}\right)\boldsymbol{\chi}_s^2\right].\\
&x^3\left[\frac{167644780815461}{8592292380672}+\left(-\frac{11327099812895}{306867585024}-\frac{205\,\pi^2}{96}\right)\eta-\frac{137763118975\,\eta^2}{1217728512}+\frac{2435519695\,\eta^3}{130470912}\right.\\
&\quad+\left(-\frac{21\,\pi}{64}+\frac{275\,\pi\,\delta}{12}+\frac{21\,\pi\,\eta}{16}\right)\boldsymbol{\chi}_a\cdot\hat{\mathbf{L}}_N+\left(\frac{32394371}{2838528}+\frac{791\,\delta}{768}+\frac{113\,\eta^2}{576}+\left(-\frac{71832779}{709632}-\frac{791\,\delta}{192}\right)\eta+\frac{59317\,\eta^2}{264}\right)\boldsymbol{\chi}_a^2.\\
&\quad+\left\{\frac{275\,\pi}{12}-\frac{21\,\pi\,\delta^3}{64}-\frac{91\,\pi\,\eta}{3}+\left(\frac{791}{768}+\frac{11114513\,\delta}{473088}-\frac{743\,\delta^3}{2688}+\frac{791\,\delta^4}{768}+\left(-\frac{77}{16}-\frac{649327\,\delta}{16896}-\frac{11\,\delta^3}{32}\right)\eta\right.\right.\\
&\quad\left.\left.+\frac{133\,\eta^2}{48}\right)\boldsymbol{\chi}_a\cdot\hat{\mathbf{L}}_N\right\}\boldsymbol{\chi}_s\cdot\hat{\mathbf{L}}_N+\left(\frac{11114513}{946176}+\frac{791\,\delta^3}{768}-\frac{743\,\delta^4}{5376}+\left(\frac{2007451}{118272}-\frac{133\,\delta^3}{192}-\frac{11\,\delta^4}{64}\right)\eta-\frac{82411\,\eta^2}{2816}\right)\boldsymbol{\chi}_s\cdot\hat{\mathbf{L}}_N\Bigg]\Bigg\}
\end{aligned}
\tag{25b}
$$

$$
\begin{aligned}
\hat{H}_{60}=-\alpha\frac{4195}{1419264\sqrt{273}}x\Bigg\{&1-\frac{3612\,\eta}{839}+x\left[-\frac{45661561}{6342840}+\frac{101414\,\eta}{2517}-\frac{48118\,\eta^2}{839}\right]+x^{3/2}\left[\frac{1248\,\pi}{839}-\frac{4992\,\pi\,\eta}{839}\right.\\
&+\left(-\frac{44}{5873}+\frac{14129\,\delta}{2517}+\left(\frac{264}{5873}-\frac{140148\,\delta}{5873}\right)\eta-\frac{352\,\eta^2}{5873}\right)\boldsymbol{\chi}_a\cdot\hat{\mathbf{L}}_N+\left(\frac{14129}{2517}-\frac{44\,\delta^3}{5873}\right.\\
&\left.+\left(-\frac{79120}{2517}+\frac{88\,\delta^3}{5873}\right)\eta+\frac{161136\,\eta^2}{5873}\right)\boldsymbol{\chi}_s\cdot\hat{\mathbf{L}}_N\Bigg]+x^{5/2}\left[\frac{66616409\,\pi}{2718360}-\frac{874693\,\pi\,\eta}{7551}+\frac{239134\,\pi\,\eta^2}{2517}+\right.\\
&\left(-\frac{8173}{634248}-\frac{1240441999\,\delta}{57085560}+\left(\frac{6479}{105714}+\frac{15116383\,\delta}{105714}\right)\eta+\left(-\frac{1100}{158571}-\frac{2406356\,\delta}{7551}\right)\eta^2-\frac{968\,\eta^3}{7551}\right)\boldsymbol{\chi}_a\cdot\hat{\mathbf{L}}_N\\
&\left.\left(-\frac{1240441999}{57085560}-\frac{8173\,\delta^3}{634284}+\left(\frac{2016684797}{14271390}+\frac{3091\,\delta^3}{317142}\right)\eta+\left(-\frac{19243010}{52857}+\frac{242\,\delta^3}{7551}\right)\eta^2+\frac{1891144\,\eta^3}{7551}\right)\boldsymbol{\chi}_s\cdot\hat{\mathbf{L}}_N\right]\\
&x^2\left[\frac{33133408041593}{1594133291520}-\frac{912563795039\,\eta}{25102880}+\frac{8054229309\,\eta^2}{25102880}-\frac{1363643519\,\eta^3}{18827160}+\left(-\frac{81}{32}+\frac{140263\,\eta}{6712}-\frac{36120\,\eta^3}{839}\right)\boldsymbol{\chi}_a^2\right.\\
&\left.+\left(-\frac{81\,\delta}{16}+\frac{73143\,\delta\,\eta}{3356}\right)\boldsymbol{\chi}_s\cdot\boldsymbol{\chi}_a+\left(-\frac{81}{32}+\frac{36991\,\eta}{3356}-\frac{7047\,\eta^2}{1678}\right)\boldsymbol{\chi}_s^2\right]
\end{aligned}
\tag{25c}
$$

$$
\hat{H}_{80}=\alpha\frac{75601}{213497856\sqrt{119}}x^2\left[1-\frac{452070\,\eta}{75601}+\frac{733320\,\eta^2}{75601}+x\left(-\frac{265354303}{33869248}+\frac{18177343651\,\eta}{321757856}-\frac{5057483259\,\eta^2}{40219732}+\frac{1828935981\,\eta^3}{20109866}\right)\right]
$$

(25d)

$$\hat{H}_{100} = -\alpha \frac{525221\, x^3}{6452379648\,\sqrt{154}} \left(1 - \frac{79841784\,\eta}{9979199} + \frac{198570240\,\eta^2}{9979199} - \frac{172307520\,\eta^3}{9979199}\right) \tag{25e}$$

We can see that all contribution to $m = 0$, even-l modes arise solely from the Christodoulou memory piece of U_{lm}. There are no hereditary-memory contribution to the radiative current multipole moments V_{lm}

We can combine the above with equation 7 and explicitly compute the memory contribution to the + waveform polarization.This can be done in the following way

$$h_{+,\times} = \frac{2\eta M x}{R} H_{+,\times} + O\left(\frac{1}{R^2}\right) \tag{26}$$

$$H_{+,\times} = \sum_{n=0}^{\infty} x^{n/2} H_{+,\times}^{(n/2)} \tag{27}$$

The memory contribution to $H_+^{n/2}$ are:

$$H_+^{(0,mem)} = \alpha \frac{1}{96} s_\Theta^2 \left(17 + c_\Theta^2\right), \tag{28a}$$

$$H_+^{(0.5,mem)} = 0, \tag{28b}$$

$$H_+^{(1,mem)} = \alpha s_\Theta^2 \left[-\frac{354241}{2064384} - \frac{62059}{1032192} c_\Theta^2 - \frac{4195}{688128} c_\Theta^4 + \eta\left(\frac{15607}{73728} + \frac{9373}{36864} c_\Theta^2 + \frac{215}{8192} c_\Theta^4\right)\right], \tag{28c}$$

$$\begin{aligned} H_+^{(1.5,mem)} = \alpha s_\Theta^2 \Bigg\{ & \left[\frac{3}{1280} + \frac{7}{3840} c_\Theta^2 + \delta\left(\frac{153}{320} + \frac{9}{320} c_\Theta^2\right) + \eta\left(-\frac{3}{320} - \frac{7}{960} c_\Theta^2\right)\right] \boldsymbol{\chi}_a \cdot \hat{\mathbf{L}}_N \\ & + \left[\left(\frac{153}{320} + \frac{9}{320} c_\Theta^2\right) + \delta\left(\frac{3}{1280} + \frac{7}{3840} c_\Theta^2\right) + \eta\left(-\frac{3}{80} + \frac{23}{240} c_\Theta^2\right) + \delta\eta\left(-\frac{3}{320} - \frac{7}{960}\right)\right] \boldsymbol{\chi}_s \cdot \hat{\mathbf{L}}_N \Bigg\} \end{aligned} \tag{28d}$$

$$\begin{aligned} H_+^{(2,mem)} = \alpha s_\Theta^2 \Bigg\{ & -\frac{3968456539}{9364045824} + \frac{570408173}{4682022912} c_\Theta^2 + \frac{122166887}{3121348608} c_\Theta^4 + \frac{7560}{15925248} c_\Theta^6 \\ & + \eta\left[-\frac{7169749}{18579456} - \frac{13220477}{18579456} c_\Theta^2 - \frac{1345405}{6193152} c_\Theta^4 - \frac{25115}{884736} c_\Theta^6\right] + \eta^2\left[\frac{10097}{147456} + \frac{5179}{36864} c_\Theta^2 + \frac{44765}{147456} c_\Theta^4\right. \\ & \left. + \frac{3395}{73728} c_\Theta^6\right] + \left[-\frac{1385}{4608} - \frac{85}{4608} c_\Theta^2 + \eta\left(\frac{19}{16} + \frac{7}{96} c_\Theta^2\right)\right] \boldsymbol{\chi}_a^2 + \left[-\frac{1385\sqrt{1-4\eta}}{2304} - \frac{85\sqrt{1-4\eta}}{2304} c_\Theta^2\right. \\ & \left. + \eta\left(\frac{\sqrt{1-4\eta}}{72} + \frac{\sqrt{1-4\eta}}{144} c_\Theta^2\right)\right] \boldsymbol{\chi}_s \cdot \boldsymbol{\chi}_a + \left[-\frac{1385}{4608} - \frac{85}{4608} c_\Theta^2 + \eta^2\left(-\frac{1}{36} - \frac{c_\Theta^2}{72}\right) + \eta\left(\frac{11}{384} + \frac{c_\Theta^2}{128}\right)\right] \boldsymbol{\chi}_s^2 \Bigg\} \end{aligned} \tag{28e}$$

$$\begin{aligned} H_+^{(2.5,mem)} = \alpha s_\Theta^2 \Bigg\{ & -\frac{2545\pi}{21504} - \frac{295\pi}{2688} c_\Theta^2 - \frac{65\pi}{7168} c_\Theta^4 + \eta\left[\frac{2545\pi}{5376} + \frac{295\pi}{672} c_\Theta^2 + \frac{65\pi}{1792} c_\Theta^4\right] + \left[\frac{11867}{3612672} + \frac{8156279\sqrt{1-4\eta}}{4816896}\right. \\ & \left. + \frac{163}{112896} c_\Theta^2 - \frac{484979\sqrt{1-4\eta}}{2408448} c_\Theta^2 + \frac{55}{1204224} c_\Theta^4 - \frac{70645\sqrt{1-4\eta}}{2064384} c_\Theta^4 + \eta^2\left(-\frac{3797}{150528} - \frac{411}{25088} c_\Theta^2\right.\right. \\ & \left.\left. + \frac{55}{150528} c_\Theta^4\right) + \eta^2\left(-\frac{3797}{150528} - \frac{411}{25088} c_\Theta^2 + \frac{55}{150528} c_\Theta^4\right) + \eta\left(-\frac{12343}{1806336} - \frac{4105391\sqrt{1-4\eta}}{10838016} - \frac{1517}{903168} c_\Theta^2\right.\right. \\ & \left.\left. + \frac{7446571\sqrt{1-4\eta}}{5419008} - \frac{55}{200704} c_\Theta^4 + \frac{58395\sqrt{1-4\eta}}{401408} c_\Theta^4\right)\right] \boldsymbol{\chi}_a \cdot \hat{\mathbf{L}}_N + \left[\frac{8156279}{4816896} + \frac{11867\sqrt{1-4\eta}}{3612672} + \frac{484979}{2408448} c_\Theta^2\right. \\ & \left. + \frac{163\sqrt{1-4\eta}}{112896} c_\Theta^2 - \frac{70645}{2064384} c_\Theta^4 + \frac{55\sqrt{1-4\eta}}{1204224} c_\Theta^4 + \eta\left(-\frac{7272431}{2709504} - \frac{12343\sqrt{1-4\eta}}{1806336} + \frac{2001211 c_\Theta^2}{1354752}\right.\right. \\ & \left.\left. - \frac{1517\sqrt{1-4\eta}}{903168} c_\Theta^2 + \frac{24725}{129024} c_\Theta^4 - \frac{55\sqrt{1-4\eta}}{200704} c_\Theta^4\right) + \eta^2\left(\frac{1965709}{2709504} - \frac{3797\sqrt{1-4\eta}}{150528} - \frac{1072289}{1354752} c_\Theta^2\right.\right. \\ & \left.\left. - \frac{411\sqrt{1-4\eta}}{25088} c_\Theta^2 - \frac{16785}{100325} c_\Theta^4 + \frac{55\sqrt{1-4\eta}}{150528} c_\Theta^4\right)\right] \boldsymbol{\chi}_s \cdot \hat{\mathbf{L}}_N \Bigg\} \end{aligned} \tag{28f}$$

(28f)

$$H_{+}^{(3,mem)} = \alpha s_{\Theta}^{2}\Bigg\{-\frac{69549014242469}{46146017820672}+\frac{6093995955001}{23073008910336}c_{\Theta}^{2}-\frac{1416977186081}{15382005940224}c_{\Theta}^{4}-\frac{2455652411}{78479622144}c_{\Theta}^{6}-\frac{9979199}{2491416576}c_{\Theta}^{8}$$
$$+\eta^{2}\left[\frac{111707903}{594542592}-\frac{792654827}{3269984256}c_{\Theta}^{2}-\frac{9226880251}{6539968512}c_{\Theta}^{4}-\frac{71269747}{148635648}c_{\Theta}^{6}-\frac{7835}{98304}c_{\Theta}^{8}\right]+\eta\left[\frac{1355497792045}{149824733184}\right.$$
$$\left.-\frac{3485\pi^{2}}{9216}-\frac{41463325921}{51502252032}c_{\Theta}^{2}-\frac{205\pi^{2}}{9216}+\frac{347235904277}{549357355008}c_{\Theta}^{4}+\frac{788232313}{3567255552}c_{\Theta}^{6}+\frac{302431}{9437184}c_{\Theta}^{8}\right]+\eta^{3}\left[\frac{10034527}{445906944}\right.$$
$$\left.+\frac{57932071}{1226244096}c_{\Theta}^{2}+\frac{29847079}{544997376}c_{\Theta}^{4}+\frac{8170691}{24772608}c_{\Theta}^{6}+\frac{9065}{131072}c_{\Theta}^{8}\right]+\left[-\frac{14443855}{66060288}+\frac{113\sqrt{1-4\eta}}{8192}+\frac{3716075}{33030144}c_{\Theta}^{2}\right.$$
$$\left.+\frac{791\sqrt{1-4\eta}}{73728}+\frac{113265}{7340032}c_{\Theta}^{4}+\eta\left(\frac{32497919}{16515072}-\frac{113\sqrt{1-4\eta}}{2048}-\frac{8200699}{8257536}c_{\Theta}^{2}-\frac{791\sqrt{1-4\eta}}{18432}c_{\Theta}^{2}-\frac{701315}{5505024}c_{\Theta}^{4}\right)\right.$$
$$\left.+\eta^{2}\left(-\frac{142301}{36864}+\frac{40501}{18432}c_{\Theta}^{2}+\frac{1075}{4096}c_{\Theta}^{4}\right)\right]\boldsymbol{\chi}_{a}^{2}+\left[\frac{4675\pi}{1152}-\frac{9\pi\sqrt{1-4\eta}}{2048}+\frac{275\pi}{1152}c_{\Theta}^{2}-\frac{7\pi\sqrt{1-4\eta}}{2048}c_{\Theta}^{2}+\eta\left(-\frac{947\pi}{288}\right.\right.$$
$$\left.\left.+\frac{9\pi\sqrt{1-4\eta}}{512}-\frac{91\pi}{288}c_{\Theta}^{2}+\frac{7\pi\sqrt{1-4\eta}}{512}c_{\Theta}^{2}\right)\right]\boldsymbol{\chi}_{s}\cdot\hat{\mathbf{L}}_{N}+\left[-\frac{14443855}{66060288}+\frac{113\sqrt{1-4\eta}}{8192}+\frac{3716075}{33030144}c_{\Theta}^{2}+\frac{791\sqrt{1-4\eta}}{73728}c_{\Theta}^{2}\right.$$
$$\left.+\frac{113265}{7340032}c_{\Theta}^{4}+\eta^{3}\left(-\frac{11}{192}-\frac{11}{384}c_{\Theta}^{2}\right)+\eta\left(\frac{15798397}{2752512}-\frac{33\sqrt{1-4\eta}}{512}+\frac{921469}{4128768}c_{\Theta}^{2}-\frac{77\sqrt{1-4\eta}}{1536}-\frac{184955}{2752512}c_{\Theta}^{4}\right)\right.$$
$$\left.+\eta^{2}\left(-\frac{9507487}{4128768}+\frac{19\sqrt{1-4\eta}}{512}-\frac{676133}{2064384}c_{\Theta}^{2}+\frac{133\sqrt{1-4\eta}}{4608}c_{\Theta}^{2}+\frac{11745}{458752}c_{\Theta}^{4}\right)\right]\boldsymbol{\chi}_{s}^{2}+\left[-\frac{9\pi}{2048}+\frac{4675\pi\sqrt{1-4\eta}}{1152}\right.$$
$$\left.-\frac{7\pi}{2048}c_{\Theta}^{2}+\frac{275\pi\sqrt{1-4\eta}}{1152}c_{\Theta}^{2}+\eta\left(\frac{9\pi}{512}+\frac{7\pi}{512}c_{\Theta}^{2}\right)+\left(\frac{113}{4096}-\frac{14443855\sqrt{1-4\eta}}{33030144}+\frac{791}{36864}c_{\Theta}^{2}+\frac{3716075\sqrt{1-4\eta}}{16515072}c_{\Theta}^{2}\right.\right.$$
$$\left.\left.+\frac{113265\sqrt{1-4\eta}}{3670016}c_{\Theta}^{4}+\eta^{2}\left(\frac{33}{128}+\frac{11\sqrt{1-4\eta}}{384}+\frac{77}{384}c_{\Theta}^{2}+\frac{11\sqrt{1-4\eta}}{768}c_{\Theta}^{2}\right)+\eta\left(-\frac{179}{1024}+\frac{56422223\sqrt{1-4\eta}}{8257536}\right.\right.\right.$$
$$\left.\left.\left.-\frac{1253}{9216}c_{\Theta}^{2}-\frac{440281\sqrt{1-4\eta}}{1376256}c_{\Theta}^{2}-\frac{17415\sqrt{1-4\eta}}{131072}c_{\Theta}^{4}\right)\right)\boldsymbol{\chi}_{s}\cdot\hat{\mathbf{L}}_{N}\right]\Bigg\} \tag{28g}$$

The effect of spin on Christodoulou memory can be seen in fig 1, which shows xH_+ as a function of x. The top left plot in fig 1 show xH_+ as a function of x for different values of dimensionless antisymmetric spin parameters χ_s values. It can be seen that with increasing the χ_s values for aligned spin case tends to increase the Christodoulou memory. It was shown by Favata [1] that increasing the PN order tends to decrease the memory contribution. For comparison we have shown the plot in Favata [1] on the top right in fig 1. The bottom plot in fig 1 show the effect of χ_s in anti aligned case.

III. MEMORY CALCULATION USING NR DATA

NR simulations most commonly output the Newman-Penrose curvature component ψ_4.The two polarization states, h_+ and $h_\times$ of the gravitational wave are related to the curvature, expressed in terms of the complex Newman-Penrose scalar ψ_4 by

$$\psi_4 = \ddot{h}_+ - i\ddot{h}_\times \tag{29}$$

Given the Newman-Penrose scalar ψ_4 for a particular mode, we have to integrate twice in time to obtain h_+ and $h_\times$. It has long been known that producing a strain, h, from the Newman-Penrose curvature component, ψ_4, typically results in a waveform with unphysical secular non-linear drift [22]. The nonlinearity of drift indicates that this is not simply a result of two constants of integration involved in transformation. This nonlinearity is potentially caused by the fact that ψ_4 is typically extracted at a finite distance from the gravitating source. The strain h is only related to ψ_4 at an infinite distance and also strictly valid in a particular gauge. As a result in NR simulation, the finite distance calculation introduces a systematic error. In simulations [23, 24], which can possibly extract truly gauge-invariant waveform at future null infinity has not able able to get rid of the secular nonlinear drift.

It has been argued in ref. [17] that an important source of unphysical non-linear drift in numerical computation of gravitational wave strain lies in the transformation of the measured data to the strain h which generally involves an integration in time. The output of the NR simulation is a discretely sampled time series of finite duration, incorporating some component of unresolved frequencies due to numerical error. This can lead to an uncontrollable non-linear drift if the integration is performed in the time domain. The method described in ref [17] gives us a way to get rid of this unphysical behavior by eliminating the lower frequencies.

The memory contribution to h_+ is given by [18]

$$h_{+}^{(mem)} \approx \frac{R}{192\,\pi}s_{\Theta}^{2}\left(17+c_{\Theta}^{2}\right)\int_{-\infty}^{T_R}|\dot{h}_{22}|^{2}dt \tag{30}$$

The above equation requires a time integration of absolute

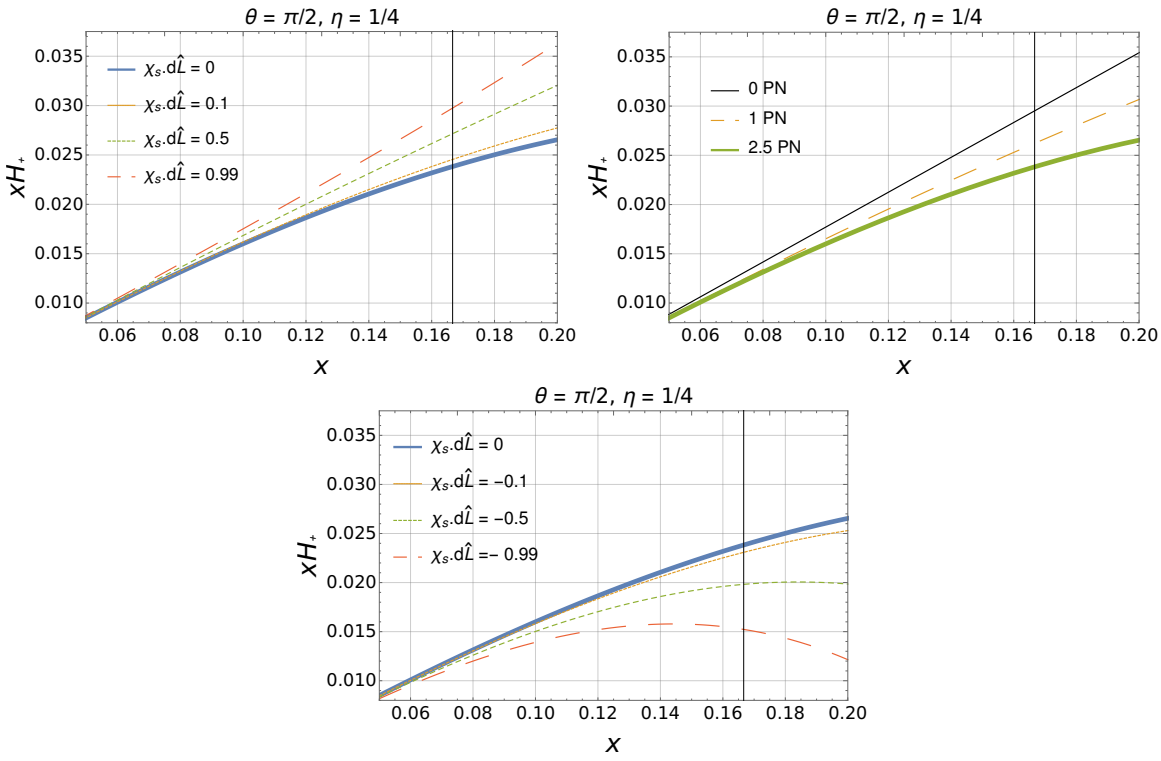

FIG. 1. Dependence of post-Newtonian (PN) corrections to the Christodoulou memory on the orbital separation. The plots above show the memory contribution to H_+ as a function of x for different dimensionless spin parameter χ values (the polar angle to the observer at $\Theta = 0$ points along the binary orbital angular momentum) for $\eta = 1/4$. The top left plot shows xH_+ as a function of parameter x which is a function of time. In plot we consider aligned spin case, where the individual spins are aligned with orbital angular momentum. It can be seen that increasing the spin magnitude tend to increase the nonlinear memory contribution. The top right figure shows the effect of including the higher PN terms to memory. this is just for comparison with Favata's results [1]. The bottom figure show the effect of spin when it is anti aligned with orbital angular momentum.

value of $\dot{h}_{22}$, but this is not typically the quantity which is directly computed in numerical simulation. The output of NR simulation is usually in the form of component of curvature tensor, or Zerilli-Moncrief-type variables defined relative to a background.

A. Evaluating Bondi News from numerical data

The Bondi News which also the first derivative of gravitational wave strain is defined as

$$\mathcal{N} = \int_{-\infty}^{t} dt' \psi_4 \tag{31}$$

The gravitational wave memory contribution to h_+ polarization can be computed from this bondi news, by integrating the absolute value of bondi news as shown in equation 30. The memory contribution evaluated using Eq.30 will contain contribution from numerical noise, which is unphysical and must be removed from the data. We apply the method described in the following section to remove the unphysical part of GW memory.

B. Integration of finite length signals in frequency domain

The unphysical part of mermory essentially lies in lower frequency. A method to remove this unphysical part is given in ref [17]. If we remove this low frequency part from the data such that the physical memory is still preserved, we can get rid of memory contribution due to numerical noise. Consider the Fourier transform, $\mathcal{F}$, applied to an absolutely integrable function $f(t)$,

$$\tilde{f}(\omega) = \mathcal{F}[f] = \int_{-\infty}^{\infty} \mathrm{e}^{-\iota\omega t} f(t) dt. \tag{32}$$

The Fourier transform of the time integral is given by

$$\mathcal{F}\left[\int_{-\infty}^{t} dt' f(t')\right]|_{\omega} = -\iota \frac{\tilde{f}(\omega)}{\omega} \tag{33}$$

The inverse fourier transform of above expression is given by

$$\int_{-\infty}^{t} dt' f(t') = \mathcal{F}^{-1}\left[-i\frac{\tilde{f}(\omega)}{\omega}\right] = -\frac{i}{2\pi}\int_{-\infty}^{\infty} \frac{1}{\omega} e^{i\omega t} \tilde{f}(\omega) d\omega \tag{34}$$

In the frequency-domain, time integration becomes a simple division by the frequency. Above method is particularly susceptible to low-frequency error, under-resolved high-frequency modes can be aliased into low-frequency modes of the signal. We try to remove these unphysical frequencies by the method described below

1. *Fixed frequency integration (FFI)*

The effect of the spurious low-frequency modes caused by spectral leakage or aliasing effects, can be significantly sup-

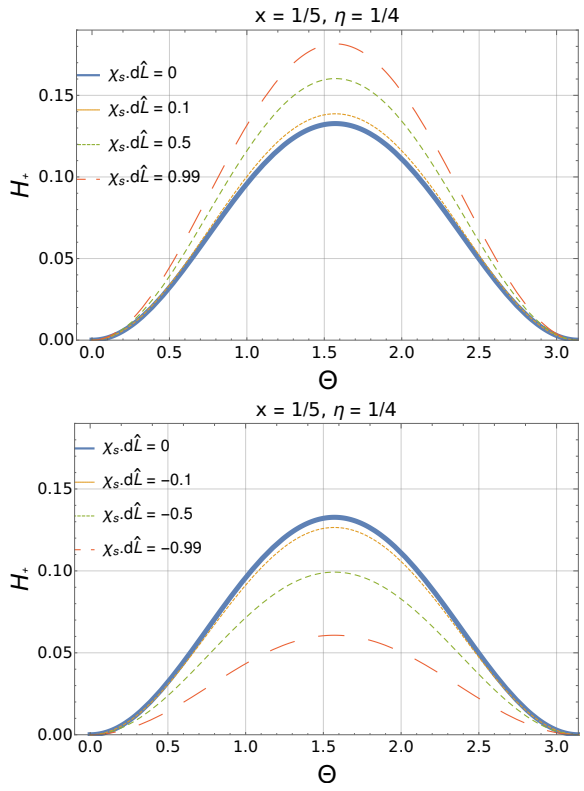

FIG. 2. Dependence of post-Newtonian (PN) corrections to the Christodoulou memory on the binary inclination and orbital separation. The plots above show the memory contribution to H_+ for different dimensionless spin parameter χ values (the polar angle to the observer at $\Theta = 0$ points along the binary orbital angular momentum) for $x = 1/5$ and $\eta = 1/4$.

pressed by use of signal filter. The time integral can be performed in frequency domain as shown in equation 34. The low frequencies which cause the unphysical nonlinear drift can be removed by choosing a cutoff frequency while taking a Fourier transform.

$$\tilde{F} = \begin{cases} -i\frac{\tilde{f}(\omega)}{\omega_0} & \omega \leq \omega_0 \\ -i\frac{\tilde{f}(\omega)}{\omega} & \omega > \omega_0 \end{cases}$$

We use this method to integrate ψ to obtain Bondi News as shown in equation 31.

C. Memory calculation from SXS Rumerical Relativity data

The publicly available SXS catalog provides data for Newman-Penrose scalar component ψ_4, decomposed into spin weighted spherical harmonics, extrapolated to infinite radius. We used this data and performed a frequency domain time integration as described in equation 34, while removing the unphysical frequency by choosing a lower cutoff as show in section III B 1. The cutoff frequency is chosen as $\omega_0/10$ where ω_0 is the minimum instantaneous GW angular frequency. We first begin by separating the complex Newman-Perose scalar ψ_4 data into phase and amplitude part. We compute instantaneous GW angular frequency from this by taking the first time derivative of phase corresponding to ψ_4. The instantaneous GW frequency often looks noisy at the beginning of the simulations due to numerical issues. We remove this noise data by choosing a lower and upper cutoff time. Once we find the upper and lower cutoff time, we can apply a frequency domain time integration for ψ_4 by choosing a cutoff frequency. After filtering the noise creating frequency we can use equation 30 to compute the memory contribution to "plus" polarization of GW signal. The SXS catalog gives data for different parameter values like mass ratio, dimensionless spin parameter etc. The Christodoulou memory computed from NR data starts from zeros using equation 30 due to finite simulation time. Chrostodoulou memory is hereditary, hence it's entire past should be included. This can be done by combining the PN expression during early inspiral and NR results for merger part. The method used to connect the memory accumulated during entire life time of BBH coalesce is described in the next section.

D. Compleate Christodoulou memory during BBH coalescence

The PN waveform for Christodoulou are given as a function of parameter x which is related to time by equation 20. This equation can be integrated to obtain a relation between time t and parameter x. The Christodoulou memory reaches it's peak value at the merger. We choose the values of integration constants such that the peak in $h_+^{(mem)}$ is reached at time $t = 0$. We use our PN results for computing the memory during early inspiral and attach them to NR results near the late inspiral. We compare this memory for different mass ratio and different values of dimensionless spin parameter. Figure 3 show the Christodoulou memory for different mass ratios, which shows that the Christodoulou tends to decrease with higher mass ratios. The effect of dimensionless spin is shown in figure 4. It can be seen that the spin magnitude has significant effect on nonlinear memory, higher spin magnitude, in case of spin aligned with orbital angular momentum tends to increase the memory contribution. When the spins are anti aligned with orbital angular momentum, it tend to decrease the Christodoulou memory. These results show that it is important to consider the spin contribution when studying the Christodoulou memory in gravitational wave signals.

IV. OBSERVING MEMORY FROM MERGER OF SUPER-MASSIVE BLACK HOLES

Nonlinear memory from the merger of super massive black hole binary can be potentially observed in pulsar timing measurement. Gravitation wave, when they pass through the space between earth and pulsar effect the time of arrival of the radio pulses at earth. The modulation in the observed frequency is given by

$$\frac{\Delta\nu}{\nu_0} = \frac{1}{2c}\int_0^D d\lambda \left(e^i e^j \frac{\partial h_{ij}}{\partial t}\right)\Big|_{path} \tag{35}$$

The pulsar timing measurement primarily measures the difference between the actual pulse arrival time and the time predicted from the spin-down model of a pulsar, which is called the timing residuals. The timing residuals $s(t)$, accumulated during a time interval of length due to passing gravitational waves is given by

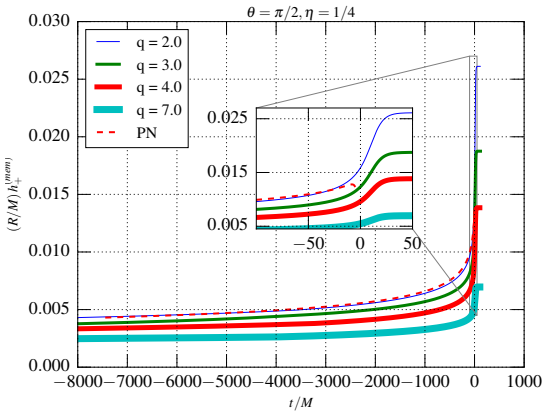

FIG. 3. The figure above shows Christodoulou memory as a function of time during BBH coalesce. This figure shows a comparison for different mass ratios. It can be seen that higher mass ration tends to decrease the Chistodoulou memory. The early inspiral part is computed using post-Newtonian expression and the later part during BBH merger is computer using NR data. The red dashed line shows result from PN expression

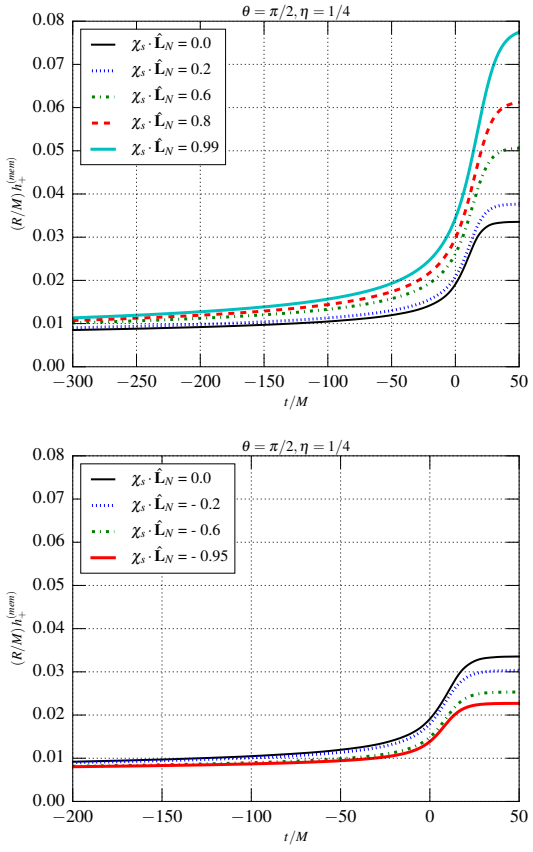

FIG. 4. The figure above shows Christodoulou memory as a function of time during BBH coalesce. The top figure shows a comparison for different values of dimensionless spin parameter χ. These results are for BBH system with equal spin magnitude for individual black hole and spins aligned with orbital angular momentum. It can be seen that higher spin magnitude tend to increase the Christodoulou memory. The bottom figure shows the anti aligned case.

the following expression

$$s(t) = \frac{1}{2}(1+\mu)\left[\left(\int_0^t d\tau\, h_+(\tau)\right)\cos 2\phi + \left(\int_0^t d\tau\, h_\times(\tau)\right)\sin 2\phi\right] \tag{36}$$

There are two unknown quantities associated with the timing residuals, the pulsar periods and it's spin down rate. We subtract these two quantities from the expression $s(t)$,

The growth in the nonlinear memory signal amplitude from super massive black hole occurs on the time scale of a few days so the effect on timing residuals can be seen if observed over a few weeks period of time. A method for observing Nonlinear memory signal from super massive black hole mergers using pulsar timing has been proposed in ref[25]. The authors have shown that the present day pulsar timing precision allows one to detect BWM due to SMBH merger at distance upto 1 Gpc (for case of equal mass 10^8 solar mass). The details regarding the calculation of the timing residuals can be seen in [25], where they consider the memory event as a step function which occurs in the middle of an observation time of 10 years. The method described in [25] is general and can be applied to case where the memory jump is not at step function. In our analysis we explore how the nonlinear memory grows during two weeks interval to time for different ranges of mass and spin parameter values. We also calculate the timing residuals as done in [25] and explore how it changes as a function of total mass and spin of black holes as shown in Fig[8].

Future observations with increased precision would be able to look at the memory growth on even shorter time of few weeks. The memory growth on the time scale of two weeks does not look like a step function, instead it's shape depends upon the spins of the merging black holes. In Fig[7].we show the memory growth interval in two weeks interval of time with solid lines for different range of spin and total mass of the binary. The dashed line show the complete memory growth in growth in geometrical units. It can be seen the as the total mass of binary becomes larger the two weeks interval of time shrinks in geometrical units. We have chosen this two weeks interval of time such that the change in memory during this time interval is maximum. For the pulsar timing observation we compute the residuals during this two week interval of time following the method described in [25]. We show a figure similar to

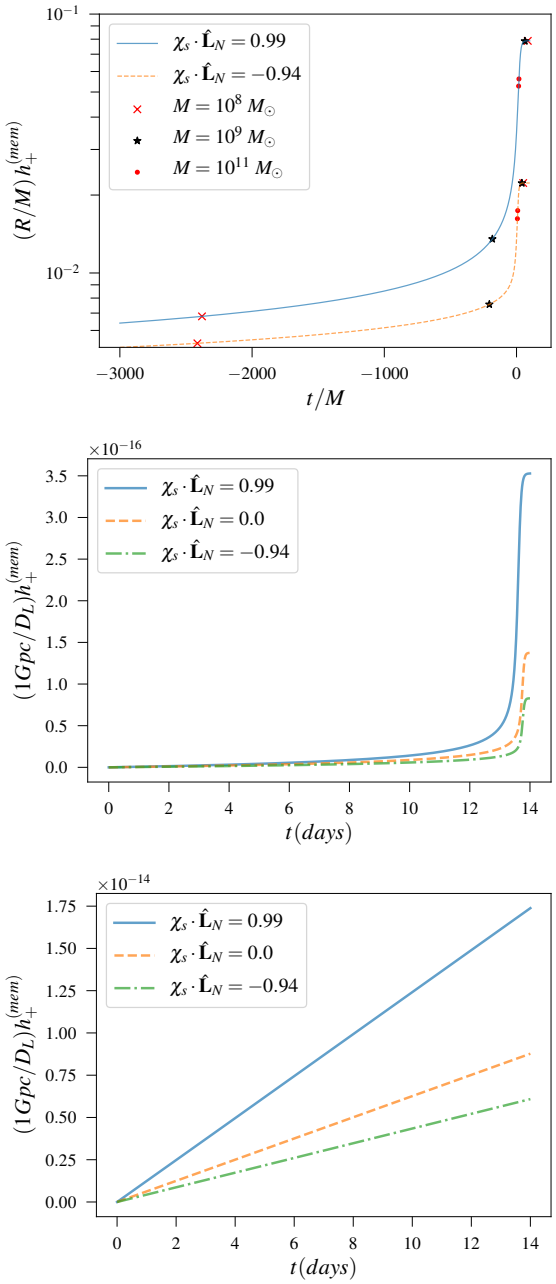

FIG. 5. The top figure shows the memory growth during merger of a binary with time measured in geometric units with total spin magnitude as indicated above. The two weeks interval of time for a given mass in indicated above. The above figure show the the memory growth in days. The left figure show this growth for $10^8 M_\odot$ and the right figure show the the memory growth in days for $10^{10} M_\odot$

V. CONCLUSIONS

Observation of Christodoulou memory would be an important test of general relativity in strong field regime. Effort to detect this memory effect in low frequency band from super massive black holes have been undertaken by pulsar timing array experiments [25]. In these experiment the spin effect have been neglected for modeling the signal. It is highly likely that super massive black holes have significant spin due to accretion of matter from surrounding. We have seen that the spin can significantly change memory amplitude as a result it can change the

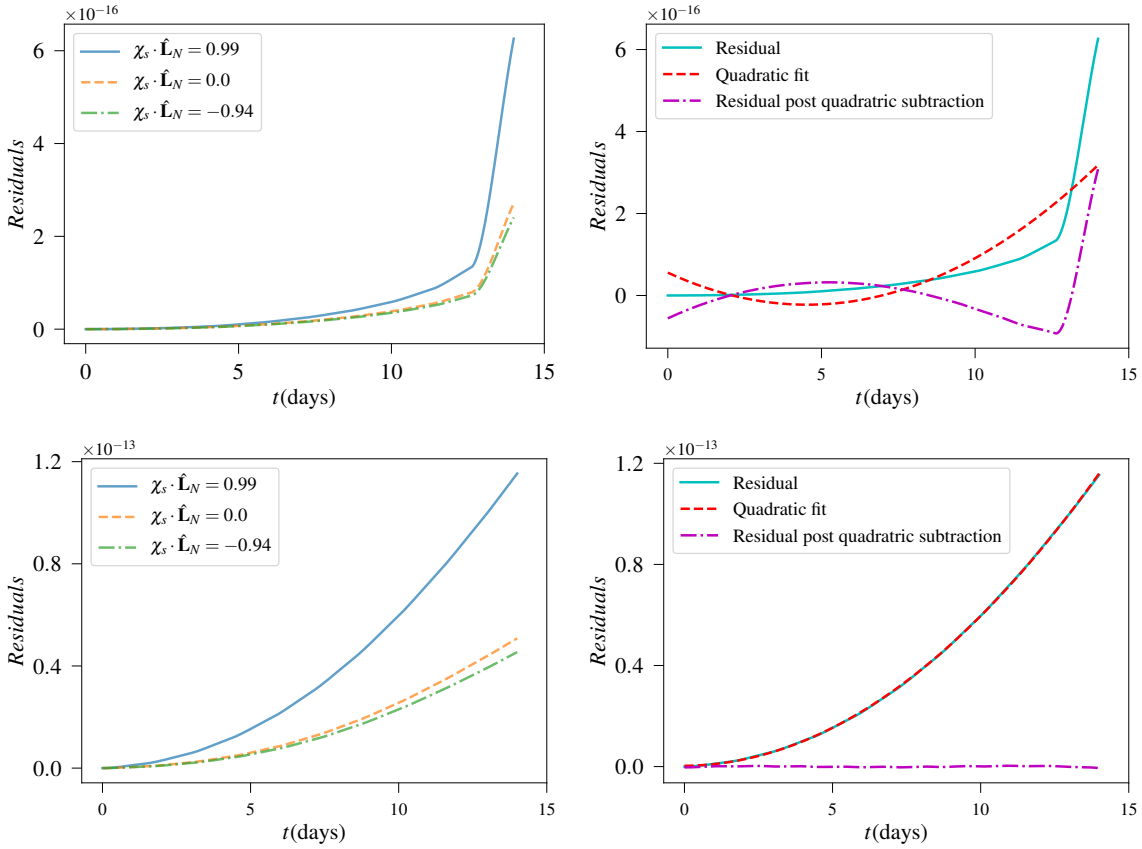

FIG. 6. The figure above shows residual growth in a given interval of time. The top left plot shows this residual growth during two weeks interval of time for different spin parameter values and the top right plot shows the residual growth after subtracting a quadratic fit for maximally spinning case and a binary with $M = 10^8\ M_\odot$. The bottom figure shows the similar plot for a binary with $M = 10^{11}\ M_\odot$.

timing residuals. Hence it is important to consider the spin effect while modeling the signals. The important thing for pulsar timing measurements would be the amount of memory changes over a single two weeks period of time which is shown the figure 8 as function of total mass of the binary and the spin magnitude. For a given mass and over the allowed spin range the net change in the memory amplitude can be as big as a factor of 5 which would change the SNR, or the expected event rate within a given volume, by a factor of $5^3 = 125$

VI. ACKNOWLEDGMENTS

We thank the West Virginia Univerisity. This work was support by ...

Appendix A: Angular Integral Of The Triple Product Of Spin-Weighted Spherical Harmonics

The following integral appears in the evaluation of nonlinear memory contribution to the radiative mass-multipole moments U_{lm}. Equation 2.4 can be rewritten as

$$d^{l_j}_{m_j s_j}(\Theta) = \sum_{k_j=k_i(j)}^{k_f(j)} g_j(k_j) \left(\sin\frac{\Theta}{2}\right)^{p_j} \left(\cos\frac{\Theta}{2}\right)^{2l_j-p_j} \tag{A1}$$

where

$$g_j(k_j) = \frac{(-1)^k_j[(l_j+m_j)!(l_j-m_j)!(l_j+s_j)!(l_j-s_j)!]^{1/2}}{k_j!(l_j+m_j-k_j)!(l_j-s_j-k_j)!(s_j-m_j+k_j)!}, \tag{A2}$$

$p_j = 2k_j + s_j - m_j$, $k_i = \max(0, m-s)$ and $k_f = \min(l+m, l-s)$. The index $j = 1, 2, 3$ serves only the three harmonics. The required integral can be written as:

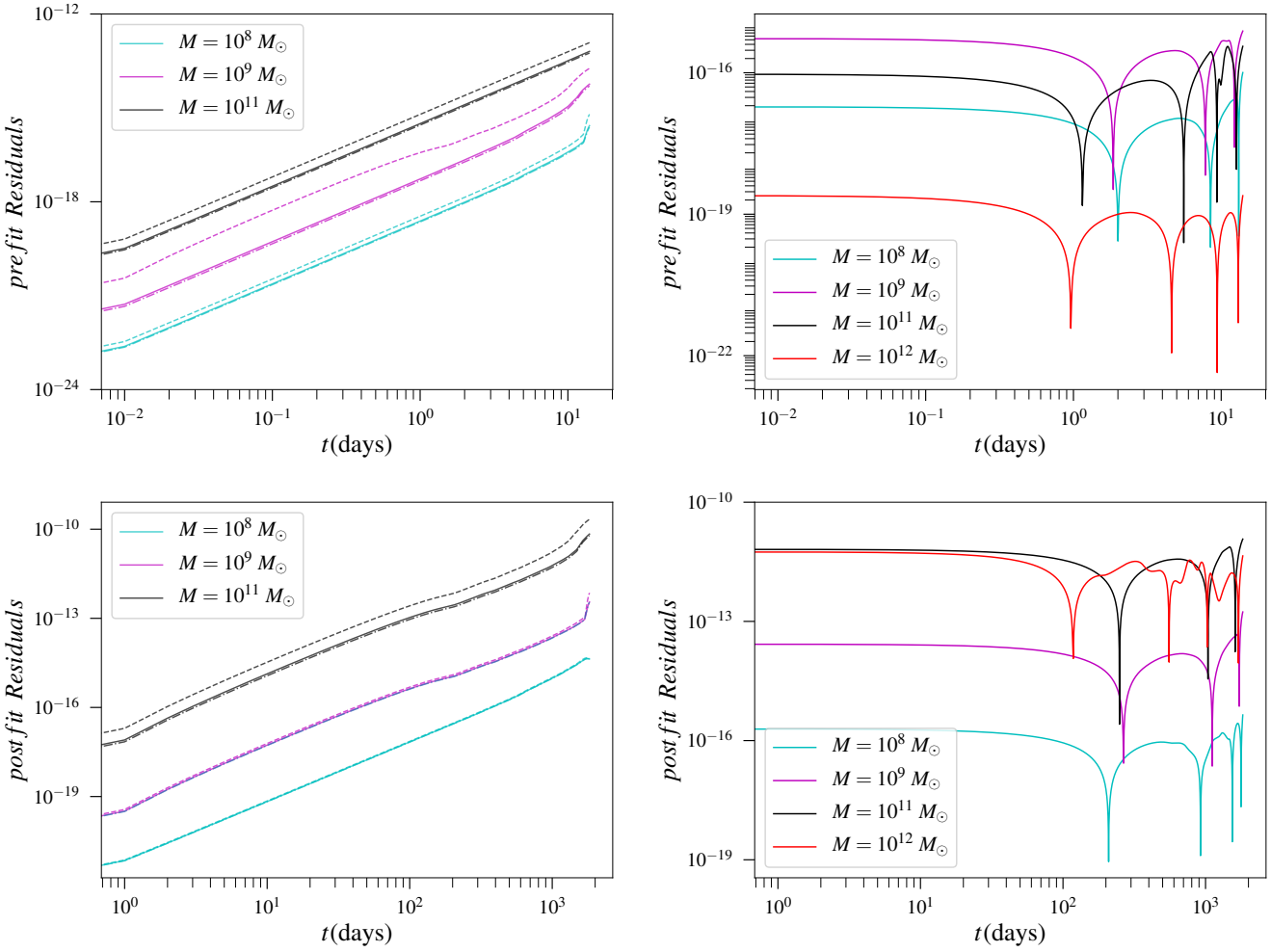

FIG. 7. The figure above shows residual growth in a given interval of time. The top left plot shows this residual growth during two weeks interval of time and the top right plot shows the residual growth after subtracting a quadratic fit. The bottom figure shows the similar plot for 5 years interval of time.

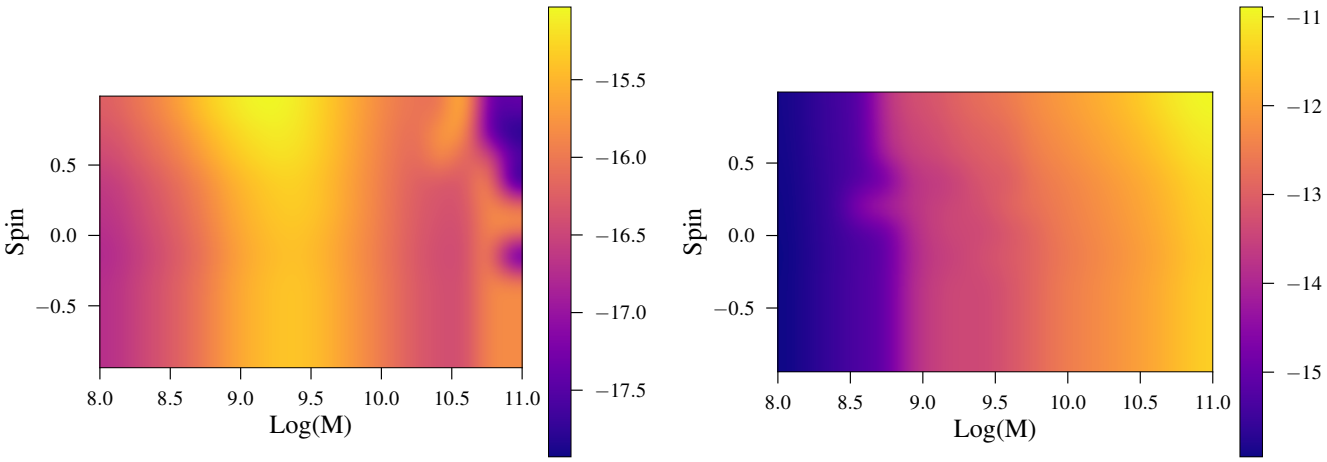

FIG. 8. The top figure shows the root mean square of post-fit timing residuals growth as a function of Mass and Spin magnitude χ. The left plot shows this post-fit residual fit during two weeks interval of time and right plot shows this for 5 years interval.

$$G^{s_1 s_2 s_3}_{l_1 l_2 l_3 m_1 m_2 m_3} \equiv \int {}_{-s1}Y^{l_1 m_1}(\Theta,\Phi)\,{}_{-s2}Y^{l_2 m_2}(\Theta,\Phi)\,{}_{-s3}Y^{l_3 m_3}(\Theta,\Phi) d\Omega$$
$$= (-1)^{s_1+s_2+s_3}\frac{[(2l_1+1)(2l_2+1)(2l_3+1)]^{1/2}}{(4\pi)^{3/2}}\int_0^{2\pi} e^{i(m_1+m_2+m_3)\Phi}d\Phi\int_0^{\pi} d^{l_1}_{m_1 s_1} d^{l_2}_{m_2 s_2} d^{l_3}_{m_3 s_3}\sin(\Theta)d\Theta \tag{A3}$$

The Φ integral is

$$\int_0^{2\pi} e^{i(m_1+m_2+m_3)\Phi}d\Phi = 2\pi\delta^{-m_1}_{m_2+m_3} \tag{A4}$$

The Φ integral can be written as

$$\int_0^{\pi} d^{l_1}_{m_1 s_1} d^{l_2}_{m_2 s_2} d^{l_3}_{m_3 s_3}\sin\Theta d\Theta = 2\sum_{k_1 k_2 k_3} g_1(k_1) g_2(k_2) g_3(k_3)\int_0^{\pi}\left(\sin\frac{\Theta}{2}\right)^{2a-1}\left(\cos\frac{\Theta}{2}\right)^{2b-1} d\Theta \tag{A5}$$

where $a = 1+(p_1+p_2+p_3)/2$ and $b = 1+l_1+l_2+l_3-(p_1+p_2+p_3)/2$. The Φ integral is expression in terms of the Beta or Gamma function and can be found in standard tables.

$$\int_0^{\pi}\left(\sin\frac{\Theta}{2}\right)^{2a-1}\left(\cos\frac{\Theta}{2}\right)^{2b-1} d\Theta = \frac{\Gamma(a)\Gamma(b)}{\Gamma(a+b)} = B(a,b) \tag{A6}$$

Appendix B: Calculation Of The $\dot{h}_{lm}$ Modes

The h_{lm} modes are written as

$$h_{lm} = 8\sqrt{\frac{\pi}{5}}\frac{\eta M}{R} x\hat{H}_{lm}(x)e^{im\psi} \tag{B1}$$

where the $\hat{H}_{lm}$ are obtained by taking the non-precessing limit of expressions for precessing binaries given in Ref.[19] . In this paper we are interested in nonprecessing case, so we rewrite the expressions such that spin are aligned with the total orbital angular momentum. The phase variable ψ is related to the orbital phase ϕ via

$$\psi = \varphi - 3x^{3/2}\left[1-\frac{\eta}{2}x\right]\ln\left(\frac{x}{x_0}\right) \tag{B2}$$

where $\ln x_0 = \frac{11}{18} - \frac{2}{3}\gamma_E - \frac{4}{3}\ln 2 + \frac{2}{3}\ln\left(\frac{M}{r_0}\right)$ is related to the arbitrary constant r_0 appearing in the coordinate transformation of Eq. (2.20) or ref[1]. The orbital phase can be expressed a function of x for nonprecessing binaries, to 3.5PN order.This expression is given in Eq(3.4) of Ref. [26]

$$\begin{aligned}\varphi(x) = -\frac{1}{32\,\eta\,x^{5/2}}\Bigg\{&1 + x\left[\frac{55\eta}{12}+\frac{3715}{1008}\right] + x^{3/2}\left[\frac{565}{24}\left(\left(1-\frac{76\eta}{133}\right)\boldsymbol{\chi}_s\cdot\hat{\mathbf{L}}_N + \delta\boldsymbol{\chi}_a\cdot\hat{\mathbf{L}}_N\right) - 10\pi\right]\\
&+ x^2\left[\left(\boldsymbol{\chi}_a\cdot\hat{\mathbf{L}}_N\right)^2\left(150\eta-\frac{3595}{96}\right) - \frac{3595\boldsymbol{\chi}_a\cdot\hat{\mathbf{L}}_N\boldsymbol{\chi}_s\cdot\hat{\mathbf{L}}_N\delta}{48} + \boldsymbol{\chi}_a^2\left(\frac{1165}{96}-50\eta\right) + \frac{1165\boldsymbol{\chi}_s\cdot\boldsymbol{\chi}_a\delta}{\delta}\right]\\
&+ \left(\boldsymbol{\chi}_s\cdot\hat{\mathbf{L}}_N\right)^2\left(-\frac{5\eta}{24}-\frac{3595}{96}\right) + \boldsymbol{\chi}_s^2\left(\frac{35\eta}{24}+\frac{1165}{96}\right) + \frac{3085\eta^2}{144} + \frac{27145\eta}{1008} + \frac{15293365}{10160664}\Bigg]\\
&+ \frac{x^{5/2}}{2}\left[\left(\boldsymbol{\chi}_a\cdot\hat{\mathbf{L}}_N\left(-\frac{35\delta\eta}{2}-\frac{732985\delta}{2016}\right) + \boldsymbol{\chi}_s\cdot\hat{\mathbf{L}}_N\left(\frac{85\eta^2}{2}+\frac{6065\eta}{18}-\frac{732985}{2016}\right) - \frac{65\pi\eta}{8}+\frac{38645\pi}{672}\right)\ln(x)\right]\\
&x^3\left[-\frac{127825\eta^3}{5184}+\frac{76055\eta^2}{6912}+\frac{2255\pi^2\eta}{48}-\frac{15737765635\eta}{12192768}-\frac{1712\gamma_E}{21}-\frac{160\pi^2}{3}+\frac{12348611916451}{18776862720}-\frac{1712\ln(16x)}{42}\right]\\
&x^{7/2}\left[-\frac{74045\pi\eta^2}{6048}+\frac{378515\pi\eta}{12096}+\frac{77096675\pi}{2032128}\right]\Bigg\}\end{aligned} \tag{B3}$$

where φ_0 is a certain reference phase. The first time derivative of modes can be obtained by using equation B1 and substituting the expression for $\dot{x}$ as a function of x using Eq. C3. We use the expression for time derivative as show in equation below

$$\dot{h}_{lm} = 8\sqrt{\frac{\pi}{5}}\frac{\eta M}{R}\dot{x}e^{-im\psi}\left(\tilde{H}'_{lm} - im\psi'\tilde{H}_{lm}\right) \tag{B4}$$

where the prime denotes the derivative with respect to x.

Appendix C: Complete 3.5 PN expressions for Energy and Flux

$$
\begin{aligned}
E = -\frac{\eta M x}{2}\Bigg\{1 + x\left[-\frac{3}{4} - \frac{\eta}{12}\right] + x^{3/2}\left[\left(\frac{8}{3} - \frac{4\eta}{3}\right)\boldsymbol{\chi}_s\cdot\hat{\mathbf{L}}_N + \frac{8}{3}\delta\boldsymbol{\chi}_a\cdot\hat{\mathbf{L}}_N\right] \\
x^2\left[-\frac{27}{8} + \frac{19\eta}{8} - \frac{\eta^2}{24} + \eta^2\left\{\left(\boldsymbol{\chi}_s^2 - \boldsymbol{\chi}_a^2\right) - 3\left[\left(\boldsymbol{\chi}_s\cdot\hat{\mathbf{L}}_N\right)^2 - \left(\boldsymbol{\chi}_a\cdot\hat{\mathbf{L}}_N\right)^2\right]\right\}\right. \\
\left.\left(\frac{1}{2} - \eta\right)\left\{\boldsymbol{\chi}_s^2 + \boldsymbol{\chi}_a^2 - 3\left[\left(\boldsymbol{\chi}_s\cdot\hat{\mathbf{L}}_N\right)^2 + \left(\boldsymbol{\chi}_a\cdot\hat{\mathbf{L}}_N\right)^2\right]\right\} + \delta\left\{\boldsymbol{\chi}_s\cdot\boldsymbol{\chi}_a - 3\left[\left(\boldsymbol{\chi}_s\cdot\hat{\mathbf{L}}_N\boldsymbol{\chi}_s\cdot\hat{\mathbf{L}}_N\right)\right]\right\}\right. \\
\left. x^{5/2}\left[\left(8 - \frac{121\eta}{9} + \frac{2\eta^2}{9}\right)\boldsymbol{\chi}_s\cdot\hat{\mathbf{L}}_N + \left(8 - \frac{31\eta}{9}\right)\delta\boldsymbol{\chi}_a\cdot\hat{\mathbf{L}}_N\right] + x^3\left[-\frac{675}{64} + \left(\frac{34445}{576} - \frac{205\pi^2}{96}\right)\eta - \frac{155\eta^2}{96} - \frac{35\eta^3}{5184}\right]\right]\Bigg\}
\end{aligned}
\tag{C1}
$$

$$
\begin{aligned}
\mathcal{L} = \frac{32}{5}\eta^2 x^5\Bigg\{1 + x\left[-\frac{1247}{336} - \frac{35\eta}{12}\right] + x^{3/2}\left[4\pi - \left\{\left(\frac{11}{4} - 3\eta\right)\boldsymbol{\chi}_s\cdot\hat{\mathbf{L}}_N + \frac{11}{4}\delta\boldsymbol{\chi}_a\cdot\hat{\mathbf{L}}_N\right\}\right] \\
x^2\left[-\frac{44711}{9072} + \frac{9271\eta}{504} + \frac{65\eta^2}{18} + \left(\frac{287}{96} + \frac{\eta}{24}\right)\left(\boldsymbol{\chi}_s\cdot\hat{\mathbf{L}}_N\right)^2 - \left(\frac{89}{96} + \frac{7\eta}{24}\right)\boldsymbol{\chi}_s^2\right. \\
\left. + \left(\frac{287}{96} - 12\eta\right)\left(\boldsymbol{\chi}_a\cdot\hat{\mathbf{L}}_N\right)^2 + \left(-\frac{89}{96} + 4\eta\right)\boldsymbol{\chi}_a^2 + \frac{287}{48}\delta\left(\boldsymbol{\chi}_s\cdot\hat{\mathbf{L}}_N\right)\left(\boldsymbol{\chi}_a\cdot\hat{\mathbf{L}}_N\right) - \frac{89}{48}\delta\left(\boldsymbol{\chi}_s\cdot\boldsymbol{\chi}_a\right)\right] \\
x^{5/2}\left[\left(-\frac{8191}{672} - \frac{583\eta}{24}\right)\pi + \left\{\left(-\frac{59}{16} + \frac{227\eta}{9} - \frac{157\eta^2}{9}\right)\boldsymbol{\chi}_s\cdot\hat{\mathbf{L}}_N + \left(-\frac{59}{16} + \frac{701\eta}{36}\delta\boldsymbol{\chi}_a\cdot\hat{\mathbf{L}}_N\right)\right\}\right] \\
\left. x^3\left[\frac{6643739519}{69854400} + \frac{16\pi^2}{3} - \frac{1712\gamma_E}{105} - \frac{856}{105}\log(16x) + \left(-\frac{134543}{7776} + \frac{41\pi^2}{48}\right)\eta - \frac{94403\eta^2}{3024} - \frac{775\eta^3}{324}\right]\right\}
\end{aligned}
\tag{C2}
$$

$$
\begin{aligned}
\frac{dx}{dt} = \frac{64x^5\eta}{5}\Bigg\{1 + x\left[-\frac{743}{336} - \frac{11\eta}{4}\right] + x^{3/2}\left[4\pi - \frac{113}{12}\delta\boldsymbol{\chi}_a\cdot\hat{\mathbf{L}}_N - \left(-\frac{113}{19} + \frac{19\eta}{3}\right)\boldsymbol{\chi}_s\cdot\hat{\mathbf{L}}_N\right] \\
+ x^2\left[\frac{34103}{18144} + \frac{13661\eta}{2016} + \frac{59\eta^2}{18} + \left(\frac{719}{96} - 30\eta\right)(\boldsymbol{\chi}_a\cdot\hat{\mathbf{L}}_N)^2 + \boldsymbol{\chi}_a^2\left(-\frac{233}{96} + 10\eta\right)\right. \\
\left. + \frac{719\boldsymbol{\chi}_a\cdot\hat{\mathbf{L}}_N\,\boldsymbol{\chi}_s\cdot\hat{\mathbf{L}}_N\delta}{48} - \frac{233\boldsymbol{\chi}_s\cdot\boldsymbol{\chi}_a\delta}{48} + (\boldsymbol{\chi}_s\cdot\hat{\mathbf{L}}_N)^2\left(-\frac{\eta}{24} - \frac{719}{96}\right) + \boldsymbol{\chi}_s^2\left(\frac{7\eta}{24} + \frac{233}{96}\right)\right] \\
+ x^{5/2}\left[-\frac{4159\pi}{672} - \frac{189\pi\eta}{8} + \boldsymbol{\chi}_a\cdot\hat{\mathbf{L}}_N\delta\left(-\frac{31319}{1008} + \frac{1159\eta}{24}\right) + \boldsymbol{\chi}_s\cdot\hat{\mathbf{L}}_N\left(-\frac{31319}{1008} + \frac{22975\eta}{252} - \frac{79\eta^2}{3}\right)\right] \\
+x^3\left[\frac{16447322263}{139708800} + \frac{16\pi^2}{3} - \frac{1712\gamma_E}{105} - \frac{56198689\eta}{217728} + \frac{451\pi^2\eta}{48} + \frac{541\eta^2}{896} - \frac{5605\eta^3}{2592} - \frac{80\pi\delta\boldsymbol{\chi}_a\cdot\hat{\mathbf{L}}_N}{3}\right. \\
+\left(\frac{575}{448} + \frac{565\delta^2}{9} - \frac{65815\eta}{4032} + \frac{89\eta^2}{2}\right)(\boldsymbol{\chi}_a\cdot\hat{\mathbf{L}}_N)^2 + \left(-\frac{145}{448} + \frac{21985\eta}{4032} - \frac{89\eta^2}{6}\right)\boldsymbol{\chi}_a^2 + \left(-\frac{80\pi}{3} + \frac{40\pi\eta}{3}\right. \\
+\delta\left(\frac{258295}{2016} - \frac{9203\eta}{96}\right)\boldsymbol{\chi}_a\cdot\hat{\mathbf{L}}_N\Big)\boldsymbol{\chi}_s\cdot\hat{\mathbf{L}}_N + \left(\frac{258295}{4032} - \frac{48773\eta}{576} + \frac{3041\eta^2}{144}\right)(\boldsymbol{\chi}_s\cdot\hat{\mathbf{L}}_N)^2 + \delta\left(-\frac{145}{224} + \frac{2143\eta}{288}\right)\boldsymbol{\chi}_s\cdot\boldsymbol{\chi}_a \\
\left.+\left(-\frac{145}{448} + \frac{1891\eta}{576} - \frac{7\eta^2}{144}\right)\boldsymbol{\chi}_s^2 - \frac{3424\,\log[2]}{105} - \frac{1712\log[x]}{210}\right]\Bigg\}
\end{aligned}
\tag{C3}
$$

REFERENCES

[1] M. Favata, Phys. Rev. D **80**, 024002 (2009), arXiv:0812.0069 [gr-qc].

[2] .

[3] D. Christodoulou, Phys. Rev. Lett. **67**, 1486 (1991).

[4] A. Burrows and J. Hayes, Phys. Rev. Lett. **76**, 352 (1996), arXiv:astro-ph/9511106 [astro-ph].

[5] E. Müller, M. Rampp, R. Buras, H. T. Janka, and D. H. Shoemaker, Astrophys. J. **603**, 221 (2004), arXiv:astro-ph/0309833

[astro-ph].
[6] C. D. Ott, Classical and Quantum Gravity **26**, 063001 (2009), arXiv:0809.0695 [astro-ph].
[7] M. B. Davies, A. King, S. Rosswog, and G. Wynn, Astrophys. J. **579**, L63 (2002), arXiv:astro-ph/0204358 [astro-ph].
[8] A. Buonanno, G. Sigl, G. G. Raffelt, H.-T. Janka, and E. Müller, Phys. Rev. D **72**, 084001 (2005), arXiv:astro-ph/0412277 [astro-ph].
[9] K. Kotake, W. Iwakami, N. Ohnishi, and S. Yamada, Astrophys. J. **697**, L133 (2009), arXiv:0904.4300 [astro-ph.HE].
[10] K. S. Thorne, Rev. Mod. Phys. **52**, 299 (1980).
[11] R. A. Isaacson, Phys. Rev. **166**, 1272 (1968).
[12] A. G. Wiseman and C. M. Will, Phys. Rev. D **44**, R2945 (1991).
[13] P. N. Payne, Phys. Rev. D **28**, 1894 (1983).
[14] L. Blanchet and T. Damour, Phys. Rev. D **46**, 4304 (1992).
[15] K. S. Thorne, Phys. Rev. D **45**, 520 (1992).
[16] D. Pollney and C. Reisswig, Astrophys. J. **732**, L13 (2011), arXiv:1004.4209 [gr-qc].
[17] C. Reisswig and D. Pollney, Classical and Quantum Gravity **28**, 195015 (2011), arXiv:1006.1632 [gr-qc].
[18] M. Favata, Classical and Quantum Gravity **27**, 084036 (2010), arXiv:1003.3486 [gr-qc].
[19] K. G. Arun, A. Buonanno, G. Faye, and E. Ochsner, Phys. Rev. D **79**, 104023 (2009), arXiv:0810.5336 [gr-qc].
[20] L. Blanchet, G. Faye, B. R. Iyer, and S. Sinha, Classical and Quantum Gravity **25**, 165003 (2008), arXiv:0802.1249 [gr-qc].
[21] L. E. Kidder, Phys. Rev. D **77**, 044016 (2008), arXiv:0710.0614 [gr-qc].
[22] E. Berti, V. Cardoso, J. A. Gonzalez, U. Sperhake, M. Hannam, S. Husa, and B. Brügmann, Phys. Rev. D **76**, 064034 (2007), arXiv:gr-qc/0703053 [gr-qc].
[23] M. Hannam, S. Husa, J. G. Baker, M. Boyle, B. Brügmann, T. Chu, N. Dorband, F. Herrmann, I. Hinder, B. J. Kelly, L. E. Kidder, P. Laguna, K. D. Matthews, J. R. van Meter, H. P. Pfeiffer, D. Pollney, C. Reisswig, M. A. Scheel, and D. Shoemaker, Phys. Rev. D **79**, 084025 (2009), arXiv:0901.2437 [gr-qc].
[24] C. Reisswig, N. T. Bishop, D. Pollney, and B. Szilágyi, Phys. Rev. Lett. **103**, 221101 (2009), arXiv:0907.2637 [gr-qc].
[25] M. S. Pshirkov, D. Baskaran, and K. A. Postnov, Monthly Notices of the Royal Astronomical Society **402**, 417 (2010), http://oup.prod.sis.lan/mnras/article-pdf/402/1/417/18581595/mnras0402-0417.pdf.
[26] P. Ajith, Phys. Rev. D **84**, 084037 (2011), arXiv:1107.1267 [gr-qc].